Physics of Fluids

Transitions between systems of satellite vortices in a rotating fluid

Cite as: Phys. Fluids **32**, 101701 (2020); https://doi.org/10.1063/5.0025030
Submitted: 13 August 2020 • Accepted: 16 September 2020 • Published Online: 01 October 2020

Giuseppe Di Labbio, Hamid Ait Abderrahmane, Mohamed Fayed, et al.

Transitions between systems of satellite vortices in a rotating fluid

Cite as: Phys. Fluids 32, 101701 (2020); doi: 10.1063/5.0025030
Submitted: 13 August 2020 • Accepted: 16 September 2020 •
Published Online: 1 October 2020

Giuseppe Di Labbio,[1] Hamid Ait Abderrahmane,[2,a)] Mohamed Fayed,[3,b)] and Hoi Dick Ng[4]

AFFILIATIONS

[1]Department of Mechanical Engineering, Polytechnique Montréal, Montréal, Quebec H3C 3A7, Canada
[2]Department of Mechanical Engineering, Khalifa University, Abu Dhabi, United Arab Emirates
[3]Mechanical Engineering Department, American University of the Middle East, Egaila 15453, Kuwait
[4]Department of Mechanical, Industrial and Aerospace Engineering, Concordia University, Montréal, Quebec H3G 1M8, Canada

[a)]**Author to whom correspondence should be addressed:** hamid.abderrahmane@ku.ac.ae
[b)]**Also at:** Department of Mechanical Power Engineering, Faculty of Engineering, Alexandria University, Alexandria, Egypt.

ABSTRACT

We investigate experimentally the transitions between systems of two and three satellite vortices found within a shallow layer of water above a rotating disk at the bottom of an open stationary cylindrical tank. We found that these systems of two and three satellite vortices are associated with two fundamental multipolar modes, namely, the quadrupole and hexapole, respectively. The forward and backward transitions between the two systems of satellite vortices, which occur at critical disk speeds, involve growth and decay of the fundamental modes as well as the excitation of their common harmonic (the dodecapole) and symmetric radial oscillations.

Swirling flows driven by a rotating disk at the bottom of an open cylindrical container are of fundamental and practical interests. They are the subject of extensive numerical and experimental studies.[1–3] The flow dynamics in such a configuration depends on two parameters, namely, the Reynolds number and the aspect ratio (fluid height to cylinder radius). At small aspect ratios, or under shallow layer conditions, the flow configuration includes two distinct regions. The inner flow region close to the axis of rotation rotates as a solid body, while the outer region near the fixed cylinder wall behaves as a shear flow. The interface between these two regions can be unstable, and its initial circular shape breaks down into azimuthal polygonal patterns. The focus of this Letter is the inner solid-body-like region, which also exhibits fascinating rotating polygonal patterns. These were reported for the first time by Vatistas in the 1990s.[4] On the one hand, these patterns are regarded as a wave phenomenon. They are explained as a result of resonance between gravity and centrifugal waves.[5] They are also described as traveling cnoidal waves, i.e., solutions of a Korteweg–de Vries equation.[6] On the other hand, the polygonal patterns are interpreted as a result of the presence of satellite vortices, symmetrically nested on a circular ring trapped within an asymmetrical and gently paraboloidal free surface.[7,8]

The transition between two subsequent polygonal patterns has previously been investigated within a wave paradigm.[9,10] The transition was found to involve a beat wave that mediates the energy transfer between the background flow and the polygonal vortex pattern. In this work, the evolution of the patterns is investigated throughout the transition between systems of satellite vortices. Specifically, we investigate the forward and backward transitions between systems of two and three satellite vortices trapped on a rotating, asymmetrical, and gently paraboloidal free surface.

The experimental setup employed in this study is the same as that described by Vatistas.[4] A shallow layer of water is brought into rotation by a rotating disk at the bottom of a stationary cylindrical tank (see Fig. 1). In the present experiments, the only control parameter is the rotation speed of the disk (Ω). For sufficiently fast rotations, the gently paraboloidal free surface deforms into elliptical and, subsequently, triangular shapes; this can be seen from the pattern formed by the seed particles floating at the free surface in Fig. 2(a).

Figures 2(b) and 2(e) show the streamlines of the raw flow fields. The wells of these surfaces, respectively, serve as traps for systems of two and three satellite vortices. These are observed in Figs. 2(c) and 2(f) after filtering out the background flow, which

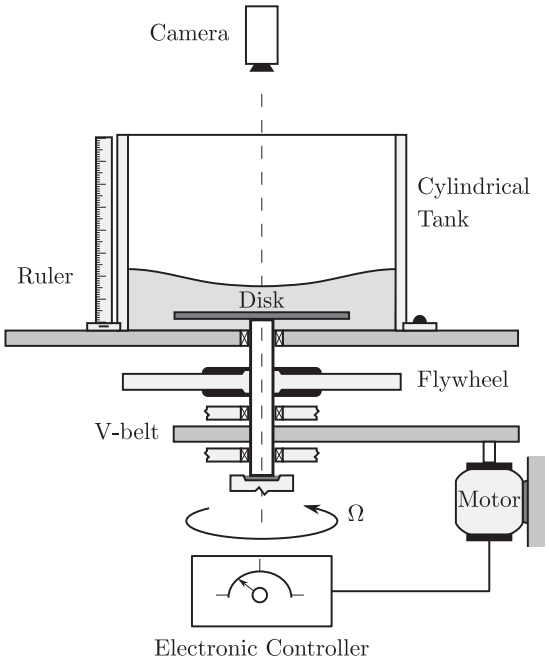

FIG. 1. Schematic of the experimental apparatus. The initial water depth, h, is 25 mm. The disk speed, Ω, is suddenly ramped up from 136 rpm to 186 rpm and maintained at this value for the forward transition (the reverse holds for the backward transition).

corresponds to the leading mode of the proper orthogonal decomposition (POD) to be discussed shortly.

The flow field at the free surface was captured using 250-μm spherical polystyrene tracer particles [white speckles floating on the free surface in Fig. 2(a)] and a high-speed camera (a resolution of 1200 × 800 pixels^2) placed above the free surface. The velocity fields were computed using PIVlab,[11] an open-source MATLAB package for particle image velocimetry. Four subsequent square windows of 64- and 32-pixel sizes with 50% window overlap were used. The field of view is circular of radius 10 cm, and the delay between frames is 25 ms. The velocity field data were then analyzed using proper orthogonal decomposition (POD).[12] Figure 3 shows the vorticity of the first few proper orthogonal modes for steady systems of two and three vortices. Mode 0 corresponds to the highest energy mode (i.e., the background flow), and the subsequent modes occur in the pairs (1, 2), (3, 4), and (5, 6), where only the first mode of each pair is shown in Fig. 3.

The structure of mode 0 is the background vorticity; it is azimuthally homogeneous in the plane perpendicular to the rotation axis. This corresponds to solid body rotation induced by the rotating disk. Fundamental pairs of oscillatory modes are also present, namely, the quadrupole and hexapole, which are associated with systems of two and three satellite vortices, respectively. As is typical of traveling structures in a flow, these modes appear in pairs having a similar kinetic energy with a slight phase difference in the azimuthal direction as well as in time. The frequencies of the steady quadrupole and hexapole are 4 Hz and 8 Hz, respectively. Interestingly, these multipolar modes appear in harmonics, namely, in pairs of $4n$-poles and $6n$-poles (n = 1, 2, 3, . . .) whose kinetic energy contributions decrease with increasing n. The superposition of the quadrupole and hexapole pairs, along with their harmonics, reproduces the two and three satellite vortex patterns, respectively. Inclusion of the background flow (mode 0) results in elliptical and triangular vorticity patches within which are nested relatively high vorticity spots; this can be seen later in Fig. 7 under the "start" and "end" headings. These spots correspond to the satellite vortices. Hence, the presence of a system of two and three satellite vortices is closely related to

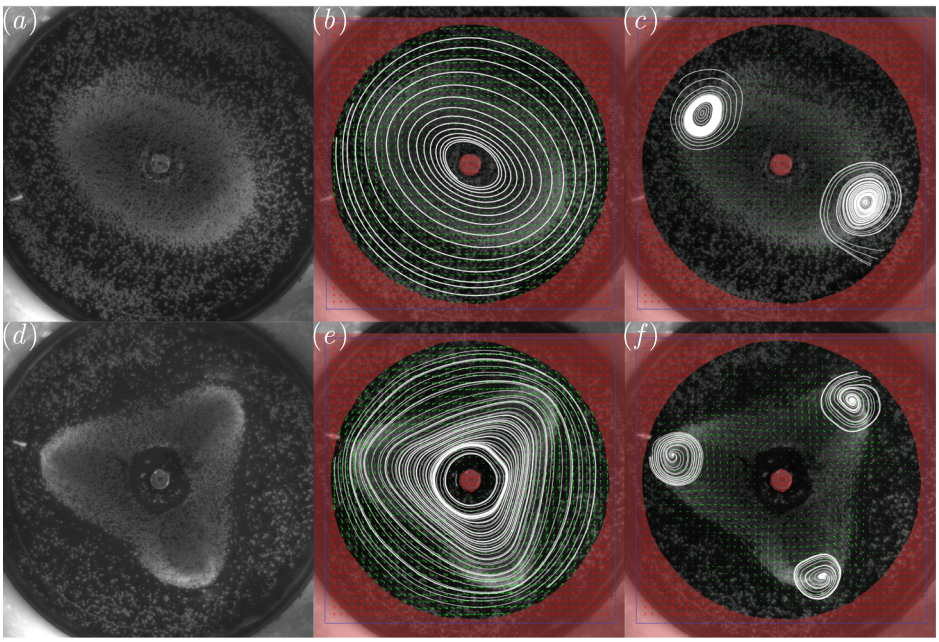

FIG. 2. [(a) and (d)] Elliptical and triangular shapes of the paraboloidal free surface revealed from the organization of the seed particles. [(b) and (e)] Corresponding streamlines of the raw flow fields for these stable patterns. [(c) and (f)] Corresponding streamlines of the satellite vortices (obtained by subtracting the leading proper orthogonal mode).

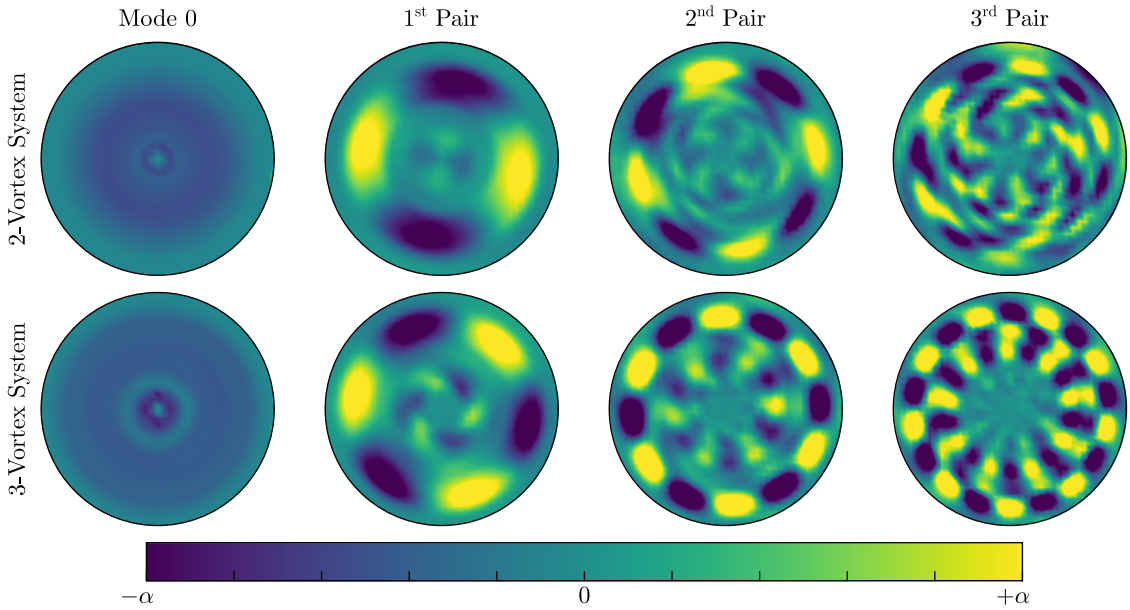

FIG. 3. Vorticity of the proper orthogonal modes for steady systems of two (top row) and three (bottom row) satellite vortices. Mode 0 corresponds to the background flow; from left to right, the absolute color bar limits (α) are 2, 3, 4, and 5. In each scenario, the pair of modes $(1, 2)$ corresponds to the quadrupole and hexapole pairs. The subsequent mode pairs occur in harmonics of the fundamental quadrupolar and hexapolar modes.

that of the fundamental quadrupolar and hexapolar modes and their harmonics, respectively.

The forward (2–3) and backward (3–2) transitions between the systems of satellite vortices occur at critical rotation speeds of the shallow water layer. The energy spectra of the respective proper orthogonal decompositions are shown in Figs. 4(a) and 4(b). In both cases, the background flow (mode 0) contains the highest energy. The first mode pair in both instances (modes 1 and 2) corresponds to the hexapoles, while the second mode pair (modes 4 and 5) corresponds to the quadrupoles. A third pair of proper orthogonal modes is also observed (modes 6 and 7 in the forward transition and modes 7 and 8 in the backward transition), which corresponds to 12-poles (i.e., dodecapoles). These are shown in Fig. 5 for both transition scenarios. The dodecapole in fact occurs as the third harmonic of the quadrupole and the second harmonic of the hexapole. Therefore, it is suspected that the dodecapole plays an important role in the transition process due potentially to a resonance-type phenomenon. It is rather peculiar that only the dodecapole is found

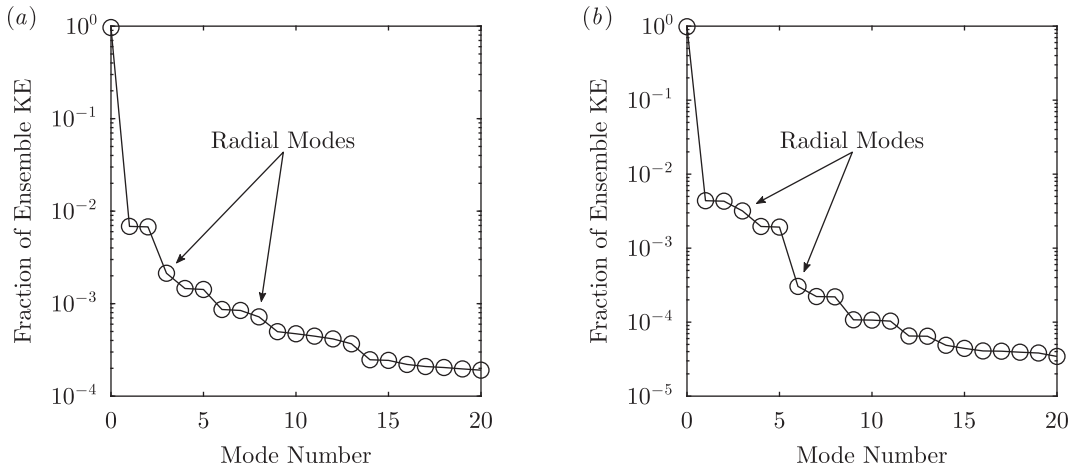

FIG. 4. Energy spectra of the proper orthogonal modes for (a) the forward transition from a system of 2–3 vortices and (b) the backward transition from a system of 3–2 vortices.

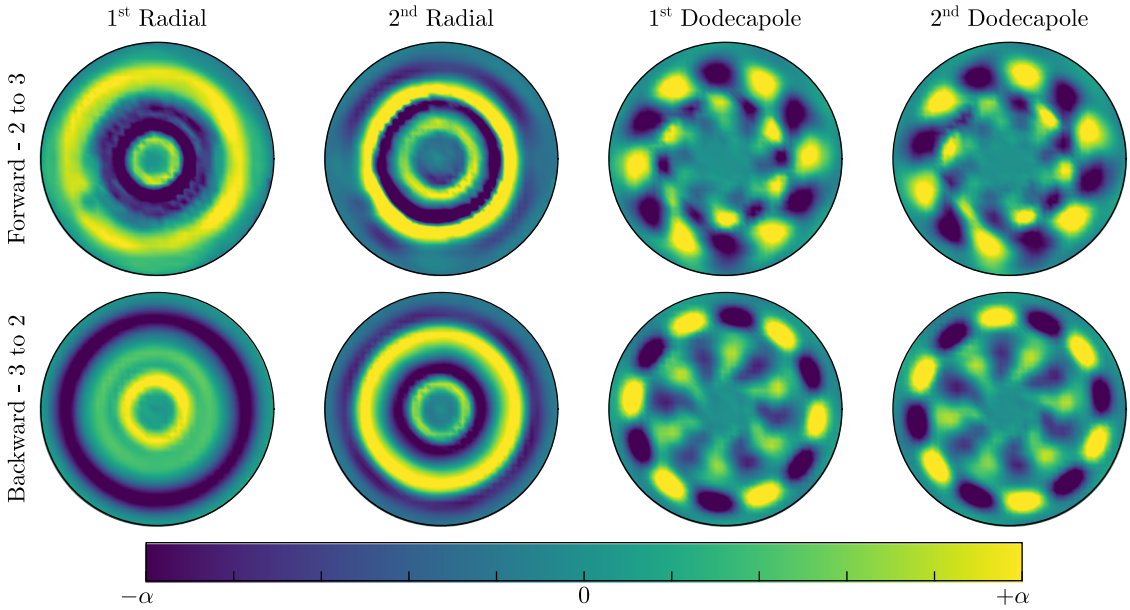

FIG. 5. Vorticity of the radial and dodecapole modes playing an important role in the transition processes between systems of 2 and 3 vortices; from left to right, the absolute color bar limits (α) are 3, 5, 5, and 5. The radial modes occur as modes 3 and 8 for the forward transition and modes 3 and 6 for the backward transition. The dodecapole pairs, respectively, occur as modes (6, 7) and (7, 8).

in the leading proper orthogonal modes of the transitions with no clear sign of the octopole or other harmonics of the quadrupole and hexapole. These other harmonics, therefore, do not play a significant role in the transition processes and are, therefore, expected to emerge only as the systems of satellite vortices stabilize. Between the hexapole and quadrupole pairs, a singular mode is also found (mode 3), which has a radial character that is closely related to the background flow. Another such mode is observed as mode 8 for the forward transition and mode 6 for the backward transition. The interpretation of higher modes (9^+) is unclear; however, their kinetic energy contributions fall off significantly. For the forward and backward transitions, modes 0–8 constitute 98.7% and 99.8% of the ensemble flow kinetic energy, respectively. Without the background flow, modes 1–8 in fact represent 61.4% and 89.8% of the ensemble flow kinetic energy, respectively. The temporal dynamics of the proper orthogonal modes for the forward and backward transitions are shown in Figs. 6(a) and 6(b), respectively. The forward transition occurs through the decay of the pair of quadrupoles and the growth of the pair of hexapoles [Fig. 6(a)]. Likewise, the backward transition occurs through the decay of the pair of hexapoles and the growth of the pair of quadrupoles [Fig. 6(b)]. The behavior of the dodecapole pair (not shown) follows closely that of the hexapole pair in both transition scenarios. The pair of dodecapoles may mediate the energy transfer between the growth and decay of the fundamental multipoles. As mentioned earlier, both the forward and backward transitions are accompanied by the excitation of radial oscillations, the temporal dynamics of which are also shown in Fig. 6.

With only the first eight modes appearing to contribute to the transition process in both scenarios, they can effectively be used as a reduced-order model to probe the transitions further. We, therefore, reconstruct the flow using the first eight modes as well as the background flow (mode 0) in both scenarios. Some illustrative moments in the forward and backward transitions are provided in Fig. 7 using the vorticity of the reconstructions. The reader is also encouraged to view videos 1–4 of the supplementary material to observe the reduced-order transitions with and without the influence of the background flow. In the case of the forward transition, the flow of course begins with two high vorticity spots, which correspond to the two satellite vortices (the first image in Fig. 7, top row). These vortices decay as they merge into the center of the background flow (second image). The background flow retains this energy until it is released as the growth of three nodes of high vorticity (third image). These high vorticity spots eventually grow to form the three satellite vortices (fourth image). In the case of the backward transition, the flow now begins with three high vorticity spots, which correspond to the three satellite vortices (the first image in Fig. 7, bottom row). These vortices decay and merge into the background flow in a similar process, creating a deformed ring of vorticity (second image). From this ring, two high vorticity regions begin to emerge very quickly (third image). These high vorticity spots eventually grow to form the two satellite vortices (fourth image). Perhaps, it is worth highlighting that the experimental conditions were set near the critical conditions and the rate at which the disk speed is varied should influence the pace at which the transitions occur. In fact, in the present experiments, the backward transition occurs faster than the forward transition. The fundamental results presented here call for further investigation with a systematic variation of the disk speed starting far from the critical conditions. Another control parameter that one should explore is the depth of the shallow water layer h.

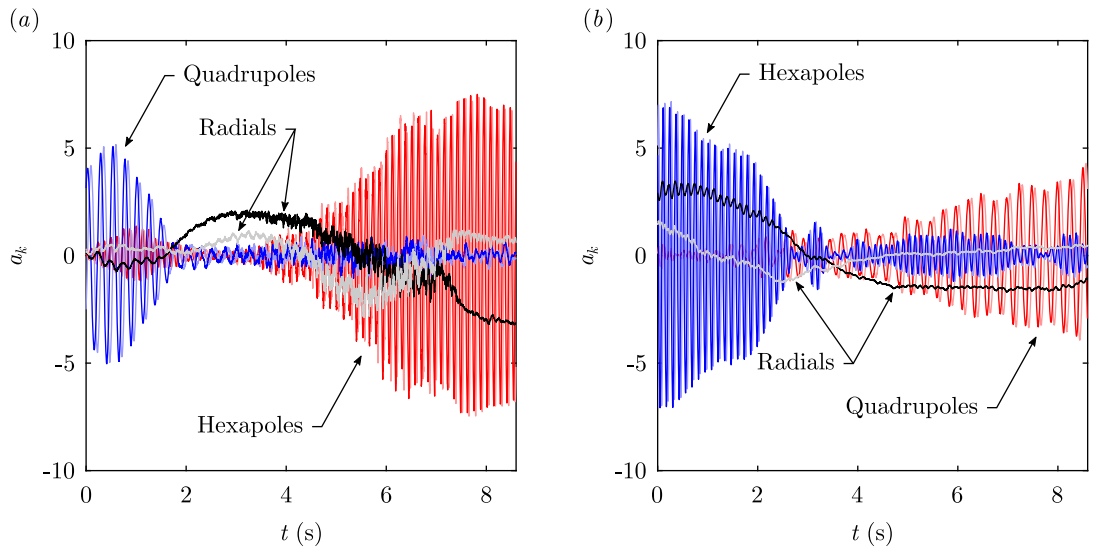

FIG. 6. Temporal dynamics of the proper orthogonal modes for (a) the forward transition from a system of 2–3 vortices and (b) the backward transition from a system of 3–2 vortices. The pairs of oscillatory quadrupoles and hexapoles are labeled, as are the two transient radial modes.

We anticipate that the variation of h will trigger similar transitions. We see such a scanning of the plane of parameters (Ω, h), in a systematic manner, as a continuation of this work. The present work can be seen as a first step toward reconciling the wave and satellite vortex approaches into a unified theory for the fascinating polygonal patterns in rotating shallow water layers in open cylinders.

In summary, we have identified the initiating mechanism that underlies the transitions between systems of satellite vortices in a stirred shallow layer of water. The mechanism is the dynamical instability of the pair of fundamental modes associated with each satellite vortex system. These fundamental modes should be the eigenstates or normal modes of the flows associated with the satellite

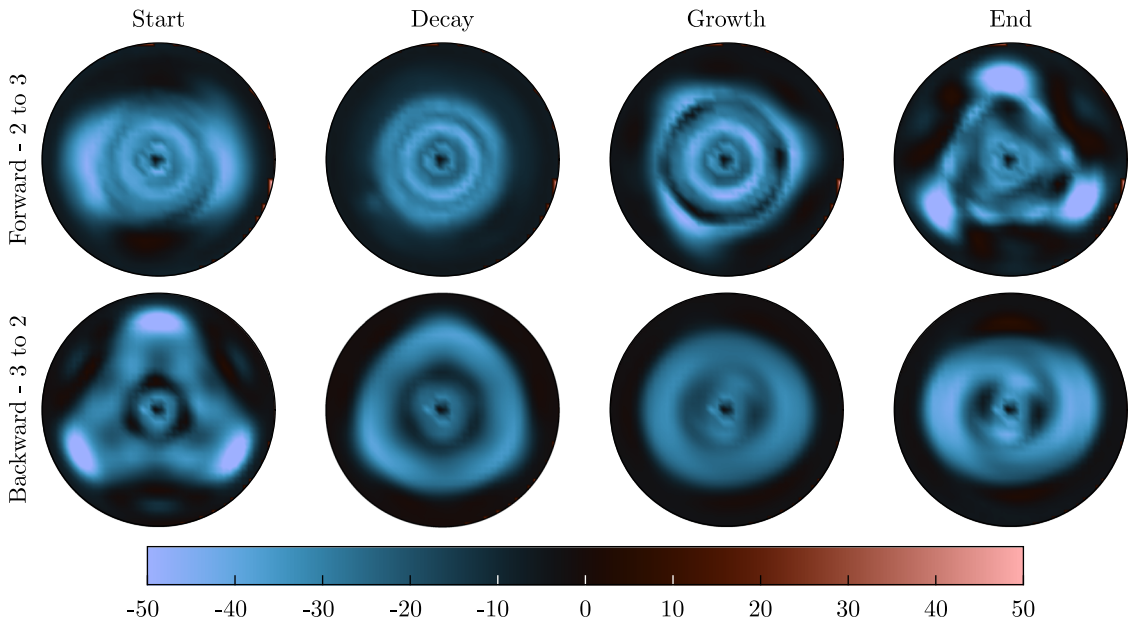

FIG. 7. Vorticity of the reduced-order models of the forward (top row) and backward (bottom row) transitions at selected instants. These instants show the starting pattern of satellite vortices, their decay, the emergence of new satellite vortices, and their subsequent growth and stabilization.

vortices trapped within the elliptical or triangular paraboloidal free surface. We believe that the instability of the quadrupole (hexapole) and its bifurcation into the hexapole (quadrupole) are due to the rapid growth of one or more eigenvalues of the evolution matrix, which maps the flows between systems of two and three satellite vortices.

See the supplementary material for four videos demonstrating the forward and backward transitions using low-order models constructed from proper orthogonal decomposition. The low-order models contain the eight leading proper orthogonal modes with or without the background flow for each transition scenario. The name of the video indicates the plotting condition by explicitly stating "with background flow" or "without background flow."

DATA AVAILABILITY

The data that support the findings of this study are available from the corresponding author upon reasonable request.

REFERENCES

[1]M. Piva and E. Meiburg, "Steady axisymmetric flow in an open cylindrical container with a partially rotating bottom wall," Phys. Fluids **17**, 063603 (2005).
[2]T. Suzuki, M. Iima, and Y. Hayase, "Surface switching of rotating fluid in a cylinder," Phys. Fluids **18**, 101701 (2006).
[3]L. Kahouadji and L. M. Witkowski, "Free surface due to a flow driven by a rotating disk inside a vertical cylindrical tank: Axisymmetric configuration," Phys. Fluids **26**, 072105 (2014).
[4]G. H. Vatistas, "A note on liquid vortex sloshing and Kelvin's equilibria," J. Fluid Mech. **217**, 241–248 (1990).
[5]L. Tophøj, J. Mougel, T. Bohr, and D. Fabre, "Rotating polygon instability of a swirling free surface flow," Phys. Rev. Lett. **110**, 194502 (2013).
[6]M. Amaouche, H. A. Abderrahmane, and G. H. Vatistas, "Nonlinear modes in the hollow-cores of liquid vortices," Eur. J. Mech.: B/Fluids **41**, 133–137 (2013).
[7]G. H. Vatistas, H. Ait Abderrahmane, and M. H. K. Siddiqui, "Experimental confirmation of Kelvin's equilibria," Phys. Rev. Lett. **100**, 174503 (2008).
[8]H. Ait Abderrahmane, M. H. K. Siddiqui, G. H. Vatistas, M. Fayed, and H. D. Ng, "Symmetrization of a polygonal hollow-core vortex through beat-wave resonance," Phys. Rev. E **83**, 056319 (2011).
[9]H. Ait Abderrahmane, M. H. K. Siddiqui, and G. H. Vatistas, "Transition between Kelvin's equilibria," Phys. Rev. E **80**, 066305 (2009).
[10]H. Ait Abderrahmane, M. Fayed, H. D. Ng, and G. H. Vatistas, "A note on relative equilibria in a rotating shallow water layer," J. Fluid Mech. **724**, 695–703 (2013).
[11]W. Thielicke and E. J. Stamhuis, "PIVlab: Towards user-friendly, affordable and accurate digital particle image velocimetry in MATLAB," J. Open Res. Software **2**, e30 (2014).
[12]L. Sirovich, "Turbulence and the dynamics of coherent structures. I. Coherent structures," Q. Appl. Math. **45**, 561–571 (1987).